

Structures and phonon properties of nanoscale fractional graphitic structures in amorphous carbon determined by molecular simulations

Tomohisa Kumagai,^{a)} Junho Choi, Satoshi Izumi, and Takahisa Kato*School of Engineering, The University of Tokyo, 7-3-1, Hongo, Bunkyo-ku, Tokyo 113-8656, Japan*

(Received 23 November 2009; accepted 16 February 2010; published online 20 May 2010)

Although amorphous carbon (a-C) materials are being widely used, relaxed atomic structures of a-C have not yet been investigated in detail. In this study, a-C structures were relaxed in molecular simulations, and their structural properties and phonon properties were investigated. As a result, several nanoscale fractional graphitic structures were observed in the annealed a-C structures. Further, it was found that the fractional graphitic structures caused a peak in the fractional phonon density of states of the annealed a-C structures, which corresponded to the D peak. The main phonon mode in the fractional graphitic structure with phonon frequencies of the D peak position and that of the G peak position were the distortion mode of six-membered rings, and the stretching mode of the bonds between threefold coordinated atoms, respectively. Both the distortion mode of six-membered rings and the bond-stretching mode were observed in phonon frequencies between the D peak position and the G peak position. © 2010 American Institute of Physics.

[doi:10.1063/1.3361334]

I. INTRODUCTION

In recent times, diamondlike carbon (DLC) films are being widely used as industrial products because of their mechanical, electronic, chemical, and biological properties.¹ The atomic structures of DLC films are amorphous carbon (a-C) networks or amorphous hydrocarbon (a-C:H) networks. Those mainly involve sp^2 and sp^3 carbon atoms and hydrogen atoms, which can be understood from a ternary phase diagram.²

As observed from a ternary phase diagram, there exist various types of a-C structures having different compositions of sp^2 and sp^3 carbon atoms and hydrogen atoms. On the other hand, it is known that there can be various amorphous states that exhibit different stabilities in the case of some amorphous materials.³ In the case of DLC films, it can be thought that there are also various amorphous states having different formation energies, even though they have the same compositions of sp^2 and sp^3 carbon atoms and hydrogen atoms. In fact, for example, the mechanical properties of DLC films were found to change by thermal annealing;⁴ the formation of graphitelike structures in an amorphous network caused moderation of the nanohardness of a-C:H structures.⁵

Molecular simulation is one of the effective methods for studying the structural relaxations in DLC films. However, relaxed atomic structures in DLC films (i.e., a-C and a-C:H structures) have not been investigated in detail by molecular simulation. By contrast, the atomic structures of as-quenched and as-deposited a-C structures have been well investigated,⁶ as have those of as-deposited a-C:H structures.⁷ Further, some structural relaxations must obviously occur in DLC films because the films are exposed to several hundred degrees Celsius during the fabrication process and to extensive use for several hours or days at room temperature.

In this study, a-C structures were selected as the target, since a-C structure is the fundamental structure in DLC films. In order to generate a-C structures that were more relaxed than as-quenched or as-deposited a-C structures, as-quenched a-C structures were subject to long-time annealing for 1 ns at high temperature in molecular simulations. Then, the structural and phonon properties of the obtained relaxed a-C structures were investigated.

Since the densities of DLC films range from 2 to 3 g/cm³ (as determined from experiments), we made relaxed a-C structures with densities of 2.0, 2.3, 2.6, 2.9, and 3.2 g/cm³. The calculations were performed using methods similar to those described in Sec. II. The obtained formation energies, which were finally evaluated by employing the environment-dependent tight-binding (EDTB) model,^{8,9} are shown in Fig. 1. Those obtained in other researches by using the tight-binding (TB) model is^{10,11} are also shown for comparison. The formation energies of a-C structures with only low densities (i.e., 2.0 and 2.3 g/cm³) were changed significantly from those of as-quenched states. On the other hand, those of the a-C structures with high densities (i.e., 2.6, 2.9, and 3.2 g/cm³) were not changed so significantly from those of the as-quenched states, because the former, whose formation energies were relatively low (Fig. 1), were already in relatively stable states. Therefore, only the results of a-C structures with a density of 2.0 g/cm³ were selected as a typical case and reported in this paper.

II. METHODS

Both liquid-quenching and annealing were performed by using classical molecular dynamics calculations. Our extended Brenner interatomic potential,¹² which was developed for reproducing a-C structures, was employed as an interatomic potential. In the potential function, a screening-type cutoff function was employed instead of a distance-

^{a)}Electronic mail: kumagai.tomohisa@fml.t.u-tokyo.ac.jp.

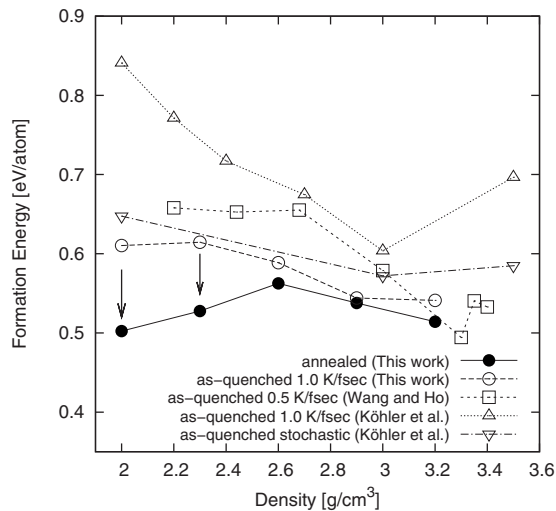


FIG. 1. Formation energies of the as-quenched a-C structures and averaged formation energies of the annealed a-C structures as a function of density evaluated by the EDTB model (Refs. 8 and 9). The averaged formation energies are averages over three cases. The formation energy is defined as the relative energy with respect to the cohesive energy of diamond. Those evaluated by the TB method in other studies (Refs. 10 and 11) are also shown for comparison. It is found that the structures and the formation energies of only the low-density (i.e., 2.0 and 2.3 g/cm³) a-C structures were changed significantly, whereas those with high densities (i.e., 2.6, 2.9, and 3.2 g/cm³) were not changed so significantly.

dependent cutoff function and a dihedral angle potential term for threefold coordinated carbon atoms was added.

In order to obtain an as-quenched a-C structure, 1000 carbon atoms placed randomly in a cubic primary cell were heated to over 8000 K and were cooled to 0 K at a rate of 2.0 K/fs. The size of the cubic primary cell was decided so that the density of the resulting a-C structure was 2.0 g/cm³. Then, the as-quenched a-C structures obtained thus were annealed at 1500 K for 1 ns. In order to accelerate the structural relaxations, the annealing temperature should be selected to be as high as possible because an energy barrier that can be overcome increases as the annealing temperature increases. However, amorphous structures melt or crystallize when the annealing temperature is too high. Therefore, the a-C structures were annealed at 1000, 1500, 2000, and 2500 K in our test calculations. The temperature of 1500 K was selected because all of the atoms in a-C structures with a density 2.0 g/cm³ formed sheetlike structures on annealing at 2000 and 2500 K. After the annealing process, the fractions of fourfold coordinated atoms in the obtained a-C structures were below 10%.

The material properties of the annealed a-C structures simulated by classical molecular dynamics calculation were evaluated by the TB method. The TB method was used because by this method, calculations can be performed for thousands of atoms and material properties can be evaluated quantitatively to some extent. In the TB method, the EDTB model proposed by Tang *et al.*^{8,9} was employed in which screening effects were introduced for constructing the TB Hamiltonian with hopping parameters and a two-body potential. This TB technique had been employed for making a-C models in another research.¹³ Only the Γ point was employed as the K point for a wave function because the atomic structure was sufficiently large.

Additional structural relaxations were performed for 10 ps at 2000 K by using TB molecular dynamics (TBMD) calculations made by employing the EDTB model because stable a-C structures obtained by using the EDTB model were different in local bonds from those obtained by using the extended Brenner interatomic potential. For both the classical molecular dynamics calculations and TBMD calculations, periodic boundary conditions were imposed on the x , y , and z directions; the time steps were of 0.3 fs; the volumes were constant; and the temperatures were controlled by velocity scaling methods. Further, in order to calculate the averaged material properties, calculations were performed for three cases. The obtained structures were called “annealed a-C structures.”

For comparison, as-quenched a-C structures with a density of 2.0 g/cm³ were also generated by employing only TBMD calculation. The cooling rate was 1.0 K/fs. Calculations were also performed for three cases for the averaged material properties. The structures obtained by this simple-quenching were called the as-quenched a-C structures.

The averaged formation energy of the annealed a-C structures and that of the as-quenched a-C structures are listed in Table I. It is found that the averaged formation energy of the annealed a-C structures was lower than that of the as-quenched a-C structures by 0.11 eV/atom.

The averaged fraction of fourfold coordinated atoms in the annealed a-C structures was 33.1%. It can be said that the atomic structures changed during structural relaxation using TBMD calculations since the fractions of fourfold coordinated atoms increased from below 10% to over 30%. Nevertheless, the required relaxed a-C structures were obtained since the annealed a-C structures had formation energies 0.11 eV/atom lower than that of the as-quenched a-C structure on

TABLE I. The averaged formation energy of the annealed a-C structures and that of the as-quenched a-C structures. The former is lower than the latter by 0.11 eV/atom due to the structural relaxations. The formation energies calculated by using TB methods in other researches are also shown for comparison. That is defined as the relative energy to the cohesive energy of diamond.

State	Annealed (this work)	As-quenched (this work)	As-quenched (Wang ^a)	As-quenched (Köhler ^b)	Stochastic (Köhler ^b)
Density (g/cm ³)	2.0	2.0	2.2	2.0	2.0
ΔE (eV/atom)	0.50	0.61	0.66	0.84	0.65

^aReference 10.

^bReference 11.

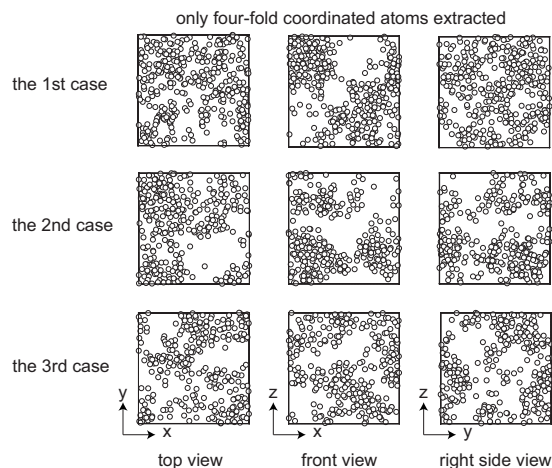


FIG. 2. Orthographic views of fourfold coordinated atoms in the annealed a-C structures. A ball indicates a fourfold coordinated atom; interatomic bonds are not shown. The coordination number of an atom was calculated by counting the number of atoms within 1.85 Å from the atom. Note that atoms that are not fourfold coordinated are not shown. It is inferred that fourfold coordinated atoms form cluster structures since regions in which fourfold coordinated atoms concentrate are clearly separated from those in which fourfold coordinated atoms are not observed.

average as shown in Table I. Further, observations of the atomic structures showed that the structural change seemed to be limited to local bond-switching.

The averaged fraction of fourfold coordinated atoms was overestimated as compared with the experimental values, which were below 20% with densities around 2 g/cm³.¹⁴ The effects of this overestimation are discussed in Sec. III.

III. STRUCTURAL PROPERTIES

The orthographic views of fourfold coordinated atoms in the annealed a-C structures of three cases are shown in Fig. 2. It was found that there were regions in which fourfold coordinated atoms were rarely observed and there were regions in which many fourfold coordinated atoms were concentrated. Therefore, it can be said that fourfold coordinated atoms formed cluster structures.

The typical atomic structures in the regions in which fourfold coordinated atoms were rarely observed were fractions of graphitelike structures. In order to investigate these structures, we define “fractional graphitic structure” as a group of sp^2 six-membered rings. An sp^2 six-membered ring means a six-membered ring that consists of only threefold coordinated atoms. Ring statistics is calculated according to the concept of the shortest-path ring.¹⁵

According to this definition, fractional graphitic structures that involve more than one sp^2 six-membered ring in the three annealed a-C structures were detected. Ball-and-stick models of them are shown in Fig. 3. It is found that fractional graphitic structures distribute in the individual cells. On the other hand, fractional graphitic structures were rarely observed in as-quenched a-C structures.

Figure 4 shows the top and side views of each fractional graphitic structure that consists of more than four sp^2 six-membered rings. The numbers of sp^2 six-membered rings in the fractional graphitic structures (a), (b), (c), (d), (e), (f), (g), (h), and (i) in Fig. 4 are 6, 9, 5, 17, 6, 5, 5, 9, and 5, respec-

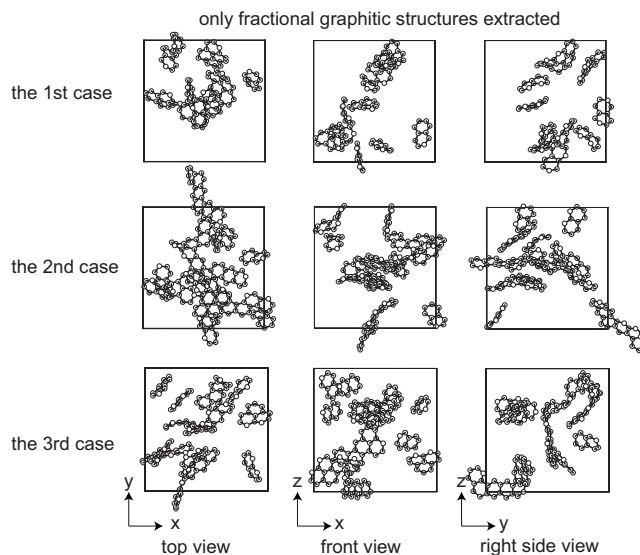


FIG. 3. Orthographic views of fractional graphitic structures that involve more than one sp^2 six-membered rings in all the three annealed a-C structures. It is observed that many fractional graphitic structures distribute in the individual cells. Note that atomic positions were shifted so that a fractional graphitic structure was not separated according to the periodic boundary conditions for the visualization.

tively. In most cases, the in-plane lengths of these fractional graphitic structures were from 0.5 to 1.5 nm. These sizes are not inconsistent with the predicted sizes [e.g., it is below 2 nm (Ref. 16)]. The exception was the largest graphitic structure in the 2nd case [i.e., (d) in Fig. 4]: The number of sp^2 six-membered rings was 17. However, this was due to the employed calculation cell size because the edge of this structure connects with the other edge through a seven-membered ring under the imposed periodic boundary condition.

In this calculation, the averaged fraction of the fourfold coordinated atoms was 33.1%, which is overestimated as compared with the fractions of sp^3 -bonded atoms determined in experiments (e.g., below 20%) as described in Sec. II.

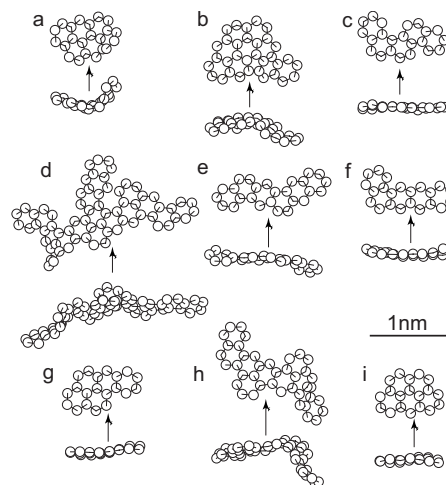


FIG. 4. Top and side views of each fractional graphitic structure that consists of more than four sp^2 six-membered rings. In most cases, the in-plane lengths of even large fractional graphitic structures ranged from 0.5 to 1.5 nm. Large fractional graphitic structures such as (a), (b), (d), (e), and (h) tended to be curved or wavy. Small fractional graphitic structures such as (c), (f), and (i) had a flat structure.

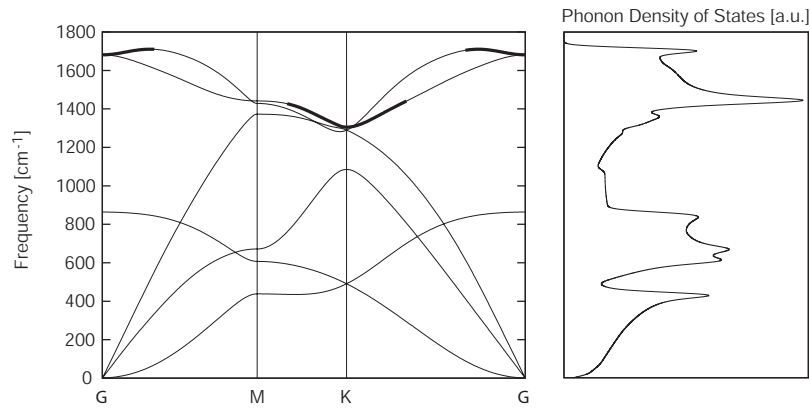


FIG. 5. Phonon dispersion of a graphene structure and PDOS calculated by using EDTB method in this work. Bold lines correspond to G peak and D peak. The PDOS was broadened by a Gaussian function with $\sigma=20$ cm^{-1} .

Therefore, if the fraction of fourfold coordinated atoms could be correctly estimated, it is thought that the in-plane lengths of the fractional graphitic structures would be slightly larger than those obtained in this calculation. However, even in such ideal calculations, fractional graphitic structures may be formed and their size may not be very different from those obtained in this calculation.

Large fractional graphitic structures tended to bend in the form of a curve or a wave, such as the structures (a), (b), (d), (e), and (h) in Fig. 4. These were bent due to the strain originating from the surrounding atoms such as fourfold coordinated atoms or atoms in five-membered rings. On the other hand, small fractional graphitic structures tended to be flat, such as the structures (c), (f), and (i) in Fig. 4.

It may be said that fractional graphitic structures were prevented from growing by other stable structures such as fourfold coordinated atoms or five-membered rings in the a-C structures. Fourfold coordinated carbon atoms are of course very stable. In addition, five-membered rings can also be said to be stable because these were the most frequent rings in the annealed a-C structures. Moreover, five-membered rings were the most frequent rings in other calculated a-C structures with a density of 2.0 g/cm^3 .^{13,17} Further, it was reported that graphitelike sheets containing five-membered rings curved into random surfaces.¹⁸

IV. PHONON PROPERTIES

With regard to experiments, it can be said that Raman analysis is suitable for evaluating the graphitic structures present in DLC films; this is because it is generally considered that the breathing mode of six-membered rings is the source of the D peak in the Raman spectra of DLC films.¹⁹ Therefore, the phonon properties of the graphitic structures are discussed because the Raman spectrum of an amorphous material can be considered to represent the phonon density of states (PDOS) weighted by an approximate matrix element.²⁰ In this study, phonon frequencies and modes were calculated as eigenvalues and eigenvectors of a dynamical matrix, respectively. Further, only the Γ point was employed as the K point.

First, in order to confirm the peak positions, the phonon dispersion of a graphene structure and PDOS were calculated

by using the EDTB method and are shown in Fig. 5. The frequencies in the phonon dispersion are slightly long as compared with those obtained from experiments or first-principles calculations (e.g., Ref. 21 and references therein) as a whole. Using the EDTB method, it is found that the D peak is around 1300 – 1450 cm^{-1} and the G peak is around 1650 – 1700 cm^{-1} since the TO mode at the K point and the LO/TO modes at the Γ point corresponded to the D peak and G peak, respectively,^{22,23} which are shown as bold lines in Fig. 5.

Fractional PDOS of the annealed a-C structures contributed by threefold coordinated atoms and that of the as-quenched a-C structures contributed by threefold coordinated atoms are shown in Fig. 6. A peak can be observed at 1420 cm^{-1} in the fractional PDOS of the annealed a-C structures while clear peaks were not observed at 1420 cm^{-1} in that of the as-quenched a-C structures. By the assignment with PDOS of a graphene structure shown in Fig. 5, it is thought that this peak at 1420 cm^{-1} corresponds to a D peak. Further, it can be said that the peak was caused by the fractional graphitic structures since the main structural difference between the annealed a-C structures and as-quenched a-C structures was the fractional graphitic structures.

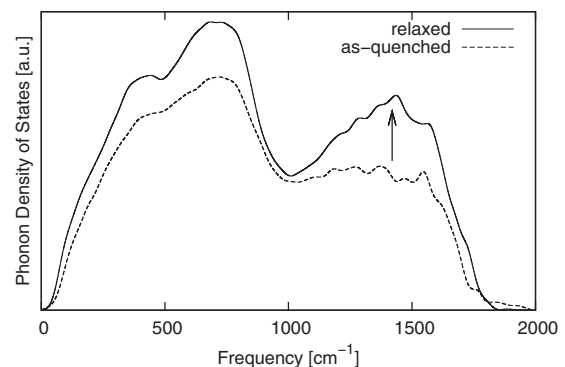


FIG. 6. Fractional PDOS contributed by threefold coordinated atoms of the annealed a-C structures and that of the as-quenched a-C structures. The peak around 1420 cm^{-1} is observed in the fractional PDOS of the annealed a-C structures, while clear peaks are not observed around 1420 cm^{-1} in the PDOS of the as-quenched a-C structures. Fractional PDOS were averaged over three cases for the annealed a-C structures and the as-quenched structures, respectively. It is noted that the PDOS were normalized (not fractional PDOSs). The normalized PDOS were broadened by a Gaussian function with $\sigma=20$ cm^{-1} .

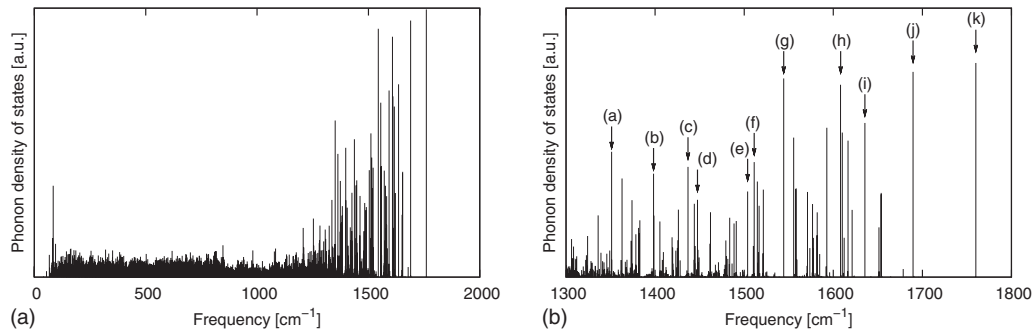


FIG. 7. The PDOS of the largest fractional graphitic structure in the 3rd case of the annealed a-C structures [i.e., (h) in Fig. 4]. The PDOS between 1300 and 1800 cm^{-1} is magnified in the figure on the right; the labels in this figure correspond to the phonon mode shown in Fig. 8. Strong phonon vibrations can be observed at frequencies exceeding 1300 cm^{-1} , while the phonon vibrations with frequencies from 0 to 1300 cm^{-1} are very weak.

In order to clarify the phonon modes of the fractional graphitic structures in the PDOS, we selected the largest fractional graphitic structure in the 3rd case of the annealed a-C structures [i.e., (h) in Fig. 4] as a sample. The PDOS of the fractional graphitic structure is shown in Fig. 7. It is found that strong phonon vibrations can be observed at frequencies exceeding 1300 cm^{-1} , while the phonon vibrations with frequencies from 0 to 1300 cm^{-1} are very weak.

Several strong phonon modes that are labeled in Fig. 7 are visualized as shown in Fig. 8. The two main types of phonon modes were found to be the stretching modes of bonds between threefold coordinated atoms and the phonon

modes caused by the distortion of the sp^2 six-membered rings. The strengths of the two modes differed according to the phonon frequency, although the two seemed to be mixed as a whole. Therefore, in order to explain the strength of the phonon modes, the frequency range is divided into three ranges for convenience: from approximately 1300 to 1450 cm^{-1} , from 1450 to 1600 cm^{-1} , and that beyond 1600 cm^{-1} .

The phonon modes in the lowest frequency range, from approximately 1300 to 1450 cm^{-1} , were mainly caused by the distortions of sp^2 six-membered rings, whereas the stretching modes of bonds between threefold coordinated atoms were not so strong. Such phonon modes may be frequently observed around the peak at 1420 cm^{-1} in the fractional PDOS of the annealed a-C structures (Fig. 6), since this range involves the frequency of the peak (i.e., 1420 cm^{-1}). The main phonon modes in this range (i.e., the distortions of sp^2 six-membered rings) can explain the fact that the peak at 1420 cm^{-1} was observed only when fractional graphitic structures were formed. It is generally considered a D peak is caused by the breathing modes of six-membered rings.¹⁹ On the other hand, in the present calculations, it can be said that the peak around 1420 cm^{-1} in the PDOS of the annealed a-C structures was caused by not only the pure breathing mode of sp^2 six-membered rings but also the distortions of these rings, although it can be thought that this peak corresponds to a D peak, as described above. However, it is natural that a pure breathing mode cannot be observed in amorphous structures, which do not have homogeneous structures. It is also considered that the reason why a D peak tends to widely distribute in the Raman spectrum of a DLC film is that the D peak is caused by not only the pure breathing mode but also various distortion modes.

The phonon modes in the highest frequency range, beyond approximately 1600 cm^{-1} , were mainly the stretching modes of bonds between threefold coordinated atoms, whereas the phonon modes that were caused by the distortions of the six-membered rings were weak. From the phonon dispersion of the graphene structure, as shown in Fig. 5, it can be said that these phonon modes correspond to a G peak. It is generally believed that a G peak is caused by the

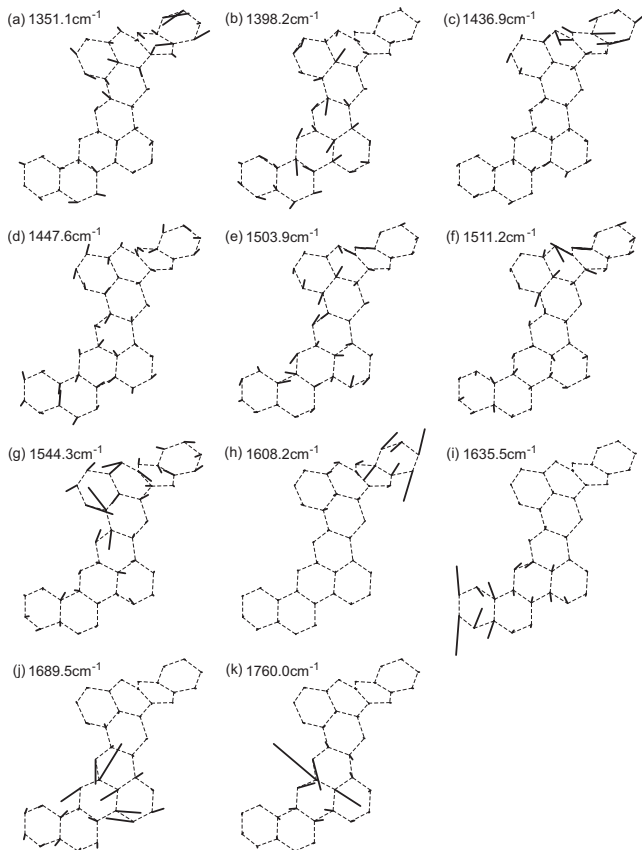


FIG. 8. Several phonon modes with strong vibrations in the largest fractional graphitic structure in the 3rd case of the annealed a-C structures [i.e., (h) in Fig. 4]. Dotted lines indicate interatomic bonds; solid lines, phonon modes.

stretching modes of sp^2 bonds.¹⁹ This predicted mode agrees with the phonon modes of frequencies beyond 1600 cm^{-1} obtained in the present calculations.

The phonon modes in the middle frequency range, between approximately 1450 cm^{-1} and approximately 1600 cm^{-1} , were both the stretching modes of bonds between threefold coordinated atoms and the distortions of sp^2 six-membered rings, which seem to be mixed. In addition, the atoms tended to vibrate along sp^2 bonds and the vibrations along sp^2 bonds became strong as the phonon frequency increased. In other words, in phonon frequencies between 1450 and 1600 cm^{-1} , the stretching mode was enhanced and the distortion mode was reduced as the phonon frequency increased.

Similar results were obtained for the phonon modes of the other fractional graphitic structures.

V. CONCLUSIONS

In this research, atomic structures and phonon properties of relaxed a-C structures were investigated. In order to generate a-C structures, three as-quenched a-C structures with a density 2.0 g/cm^3 were annealed at 1500 K for 1 ns. The annealing was simulated by using classical molecular dynamics simulations employing an extended Brenner potential. The material properties were evaluated by the EDTB method.

In the annealed a-C structures, several fractional graphitic structures were observed. The in-plane lengths of the fractional graphitic structures were between 0.5 and 1.5 nm in most cases. These sizes are not inconsistent with those predicted from experiments. Further, large fractional graphitic structures tended to be curved or waved, while small ones tended to be flat. It was found that the fractional graphitic structures caused a peak in the fractional PDOS of the annealed a-C structures, which corresponded to the D peak. The main phonon mode in the fractional graphitic structure with frequencies of the D peak position and that of the G peak position were the distortion mode of six-membered rings, and the stretching mode of bonds between threefold coordinated atoms, respectively. Further, the distortion modes and the bond-stretching modes seemed to be mixed with phonon frequencies between the D peak position and

the G peak position. In the phonon modes with these intermediate phonon frequencies, the stretching mode was enhanced and the distortion mode was reduced as the phonon frequency increased.

ACKNOWLEDGMENTS

This study was supported by a Grant-in-Aid for Young Scientists (B) Grant No. 20760065 from MEXT and a Grant-in-Aid for Scientific Research (A) Grant No. 20246034 from KAKENHI.

- ¹J. Robertson, *Mater. Sci. Eng. R.* **37**, 129 (2002).
- ²W. Jacob and W. Möller, *Appl. Phys. Lett.* **63**, 1771 (1993).
- ³E. P. Donovan, F. Spaepen, D. Turnbull, J. M. Poate, and D. C. Jacobson, *J. Appl. Phys.* **57**, 1795 (1985).
- ⁴W. Zhang, A. Tanaka, K. Wazumi, Y. Koga, and B. S. Xu, *Diamond Relat. Mater.* **13**, 2166 (2004).
- ⁵S. V. Singh, M. Creatore, R. Groenen, K. Van Hege, and M. C. M. van de Sanden, *Appl. Phys. Lett.* **92**, 221502 (2008).
- ⁶N. A. Marks, *J. Phys.: Condens. Matter* **14**, 2901 (2002), and references therein.
- ⁷E. Neyts, M. Eckert, and A. Bogaerts, *Chem. Vap. Deposition* **13**, 312 (2007).
- ⁸M. S. Tang, C. Z. Wang, C. T. Chan, and K. M. Ho, *Phys. Rev. B* **53**, 979 (1996); *Phys. Rev. B* **54**, 10982(E) (1996).
- ⁹C. Z. Wang and K. M. Ho, in *Handbook of Materials Modeling*, edited by S. Yip (Springer, The Netherlands, 2005), pp. 307–347.
- ¹⁰C. Z. Wang and K. M. Ho, *Phys. Rev. B* **50**, 12429 (1994).
- ¹¹Th. Köhler, Th. Frauenheim, and G. Jungnickel, *Phys. Rev. B* **52**, 11837 (1995).
- ¹²T. Kumagai, S. Hara, J. Choi, S. Izumi, and T. Kato, *J. Appl. Phys.* **105**, 064310 (2009).
- ¹³R. Haerle, E. Riedo, A. Pasquarello, and A. Baldereschi, *Phys. Rev. B* **65**, 045101 (2001).
- ¹⁴S. Ravi, P. Silva, Shi Xu, B. X. Tay, H. S. Tan, and W. I. Milne, *Appl. Phys. Lett.* **69**, 491 (1996).
- ¹⁵D. S. Franzblau, *Phys. Rev. B* **44**, 4925 (1991).
- ¹⁶J. Schwan, S. Ulrich, V. Batori, H. Ehrhardt, and S. R. P. Silva, *J. Appl. Phys.* **80**, 440 (1996).
- ¹⁷N. A. Marks, N. C. Cooper, D. R. McKenzie, D. G. McCulloch, P. Bath, and S. P. Russo, *Phys. Rev. B* **65**, 075411 (2002).
- ¹⁸S. J. Townsend, T. J. Lenosky, D. A. Muller, C. S. Nichols, and V. Elser, *Phys. Rev. Lett.* **69**, 921 (1992).
- ¹⁹A. C. Ferrari and J. Robertson, *Phys. Rev. B* **61**, 14095 (2000).
- ²⁰R. Alben, D. Weaire, J. E. Smith, and M. H. Brodsky, *Phys. Rev. B* **11**, 2271 (1975).
- ²¹L. Wirtz and A. Rubio, *Solid State Commun.* **131**, 141 (2004).
- ²²M. J. Matthews, M. A. Pimenta, G. Dresselhaus, M. S. Dresselhaus, and M. Endo, *Phys. Rev. B* **59**, R6585 (1999).
- ²³S. Piscanec, M. Lazzeri, F. Mauri, A. C. Ferrari, and J. Robertson, *Phys. Rev. Lett.* **93**, 185503 (2004).